Numerical Simulation on Liquid Hydrogen Chill-down Process of Vertical Pipeline

Yutaka UMEMURA
Japan Aerospace eXploration Agency, 2-1-1 Sengen, Tsukuba, Ibaraki, 305-8505, JAPAN

Takehiro HIMENO
University of Tokyo, 7-3-1 Hongo, Bunkyo-ku, Tokyo, 113-8656, JAPAN

Kiyoshi KINEFUCHI, Yasuhiro SAITO
Japan Aerospace eXploration Agency, 2-1-1 Sengen, Tsukuba, Ibaraki, 305-8505, JAPAN

Jason W. Hartwig, Daniel M. Hauser, Barbara Sakowski, and Wesley L. Johnson
NASA Glenn Research Center, 21000 Brookpark Rd, Cleveland, OH 44135, U.S.A.

Andre C. LeClair
NASA Marshall Space Flight Center, Huntsville, AL 35812, U.S.A.

and

Osamu FUKASAWA
Ryoyu System Co., 3-7-3 Uchiyama, Chikusa-ku, Nagoya, 464-0075, JAPAN

In order to improve the cryogenic propellant management technologies for a liquid hydrogen rocket with high specific impulse, JAXA, the University of Tokyo, and the NASA Glenn Research Center have jointly organized a multi-agency model validation collaboration project. As part of this project, JAXA's boiling simulation was validated with NASA's experimental data on vertical pipeline chill-down. Simulation results were in good agreement with the experimental data obtained using an improved boiling model to reproduce the spray flow. This activity achieved liquid hydrogen turbo-pump simulation at JAXA for grasping the boiling flow phenomenon from engine cut-off to re-ignition. This joint research resulted in an international cooperative relationship for discussing the cryogenic propellant management technologies necessary to develop next-generation liquid rockets.

Nomenclature

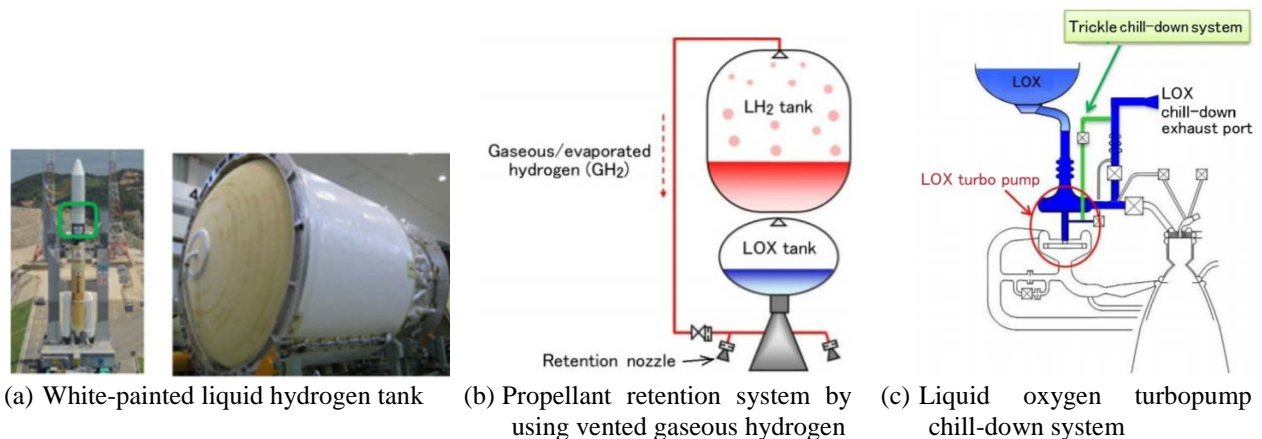|		
t	=	Time [s]
ρ	=	Density [kg/m^3]
$\vec{u}$	=	Velocity [m/s]
e	=	Internal energy [J/kg]
T	=	Static temperature [K]
P	=	Static pressure [Pa]
φ	=	Distance function from interface [m]
$\vec{q}$	=	Heat flux [W/m^2]
C_p	=	Specific heat at constant pressure [J/kg/K]
C_S	=	Sound velocity [m/s]
μ	=	First viscosity coefficient [Pa·s]
λ	=	Second viscosity coefficient [Pa·s]
k	=	Thermal conductivity [W/m/K]
σ	=	Surface tension [N/m]
$\vec{n}$	=	Normal vector at the interface [-]
δ_S	=	Dirac's delta function [1/m]
L	=	Latent heat [J/kg]
∇	=	Nabla operator [1/m]

I. Introduction

IN 2015, the mission capabilities of Japan's flagship rocket H-IIA were upgraded for the vehicle's injection into geostationary transfer orbit (GTO). In this upgrade project, the coasting duration of the H-IIA upper stage was enhanced from one to five hours by improving cross-cutting cryogenic propulsion technologies [1]. These improved technologies entailed reducing propellant vaporization by a white-painted liquid hydrogen tank, adapting propellant retention by using vented gaseous hydrogen, and improving liquid oxygen turbopump chill-down operation.

The white-painted liquid hydrogen tank was an improvement to reduce heat flux due to radiation. The liquid hydrogen tank cylinder had been wrapped in polyisocyanurate foam to prevent heat exchange with the atmosphere. The tank cylinder was colored orange before the upgrade to match the color of the material itself. Simply reducing liquid hydrogen evaporation in the tank is an inadequate measure to realize a long coasting flight. Therefore, applying a coat of white paint on the surface achieved the effect of lowering the outer surface temperature of the cylinder.

The retention of propellant was conducted to settle liquid propellant at the bottom of the tank by adding low acceleration under zero gravity in the upper stage rocket. Before the upgrade, low acceleration had been obtained by reaction control systems using hydrazine. This improvement adopted a method of converting the discharge reaction of evaporated gas in the hydrogen tank into thrust, thereby promoting the effective utilization of propellant and avoiding the additional load of a hydrazine tank.

The turbopump chill-down operation is necessary to restart engine ignition for avoiding large evaporation inside the turbopump because the turbine reaches a high temperature during engine operation. The turbopump was chilled internally by a flow of cryogenic propellant. However, such propellant was not used to obtain a thruster impulse. Thus, the mass flow rate used to chill-down the turbopump internally had to be minimized by adding a drain line as shown in Fig. 1.1. Moreover, it is necessary to understand the boiling phenomenon of low mass flow under low gravity in order to optimize the propellant consumption for turbopump chill-down operation. Given the complex boiling flow in a turbopump during the chill-down process, however, it had been difficult to evaluate said boiling flow phenomenon in advance due to a lack of knowledge and simulation technology. Therefore, JAXA and the University of Tokyo conducted a sub-scale model experiment by using a sounding rocket and developing a boiling simulation tool to improve the situation. One objective of these activities was to clarify the liquid oxygen boiling phenomena. The improvement of chill-down operation entailed reducing the mass flow of liquid oxygen (having density 16 times greater than that of liquid hydrogen) to reduce the inert weight of the upper stage, while maintaining the mission success rate. Based on the above background, JAXA and the University of Tokyo jointly conducted research on a boiling simulation tool development as shown in Fig. 1.2, and JAXA evaluated the liquid oxygen turbopump chill-down process under a low gravity environment.

As a result of the upgrade project, the H-IIA launch vehicle flight No. 29 successfully made a long-term coasting flight and three re-ignitions, and injected the Telstar 12 Vantage satellite into GTO. And it is now possible to evaluate the thermal flow phenomena of the upper stage system as shown in Fig. 1.5 due to the post-flight evaluation for checking the effects of adapting the new propellant management technologies. Consequently, JAXA must determine whether the experience and knowledge gained in this upgrade project, which has adapted many improvements in propellant management technologies, will be applied to next-generation rocket development.

(a) White-painted liquid hydrogen tank (b) Propellant retention system by using vented gaseous hydrogen (c) Liquid oxygen turbopump chill-down system

Fig. 1.1. Improved components of propellant management technologies in the H-IIA upgrade project [1]
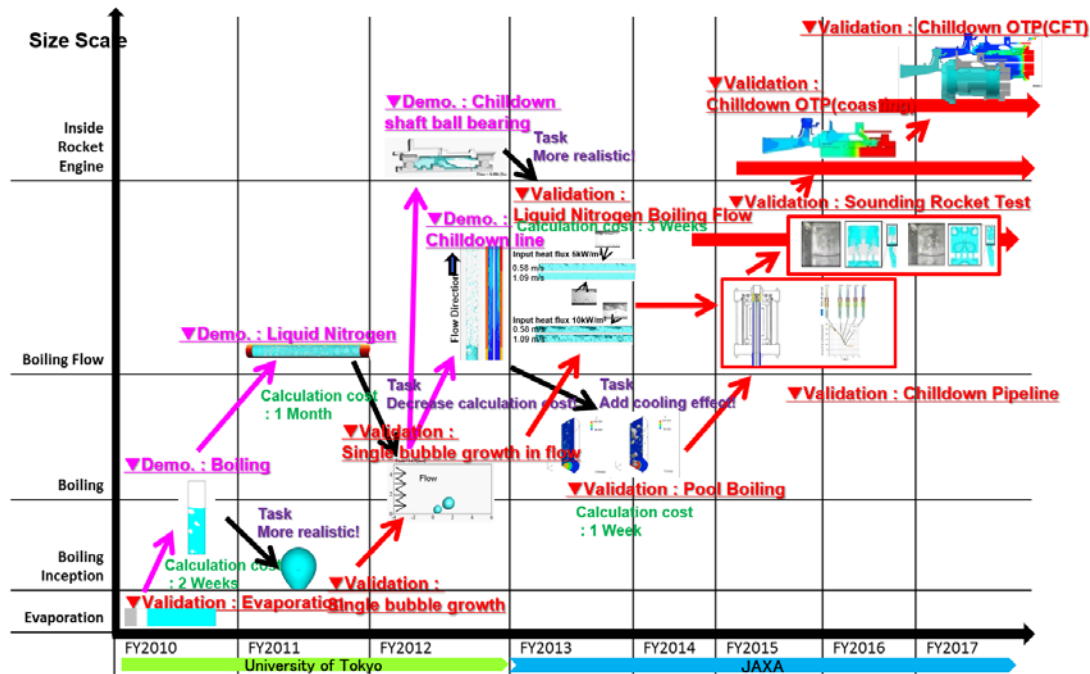
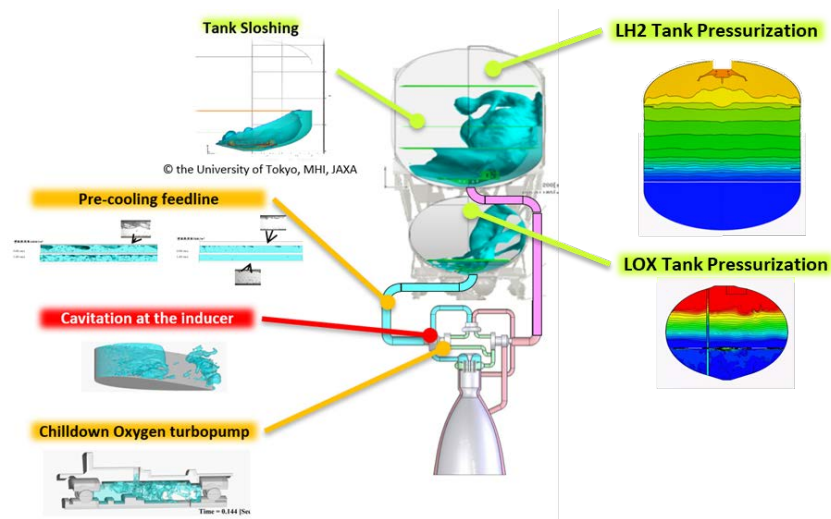**Fig. 1.2. History of oxygen boiling simulation**

Fig. 1.3. Simulation of propellant management for the H-IIA upper stage

In the current era where liquid rockets such as SpaceX are being reused, the keywords of next-generation liquid rocket development have become "orbital transportation by large impulse" and "cost reduction." Among the technologies that respond to these keywords, propellant management technologies, such as multiple ignitions of an engine, must be continuously upgraded. For example, to reuse a booster stage rocket on Earth, multiple re-ignitions are required to return with a minimal flight path. Furthermore, re-ignition for a flight-back burn is required in a short time, in order to return the rocket near the launching point. It is thus necessary to improve such engine re-ignition conditions as turbopump chill-down in order to satisfy this requirement with a liquid hydrogen engine with high specific impulse.

It is usually reasonable to conduct a captive firing test for acquiring turbopump chill-down data in an experiment. This is because a very large amount of heat is required to reproduce the temperature distribution inside the turbopump. However, it is difficult to install many temperature sensors for grasping internal thermal flow phenomena due to the presence of rotating parts inside the turbopump. Therefore, turbopump chill-down simulation

3

American Institute of Aeronautics and Astronautics

has been expected to help us understand such phenomena. As JAXA has yet to complete the validation of the liquid hydrogen chill-down process, it has aimed to realize an evaluation technology for the liquid hydrogen chill-down process by using and applying the experience and knowledge gained from simulation tool development in the H-IIA upgrade project. In boiling simulation development, it was important to validate the pipeline chill-down experiment in order to check the chilling rate and pressure loss. JAXA aimed to realize the liquid hydrogen chill-down evaluation technology based on the chill-down pipeline data provided from the NASA Glenn Research Center in collaborative research on the modeling for propellant management.

II. Research Purpose

In this research, the ultimate objective is to realize chill-down simulation of a liquid hydrogen turbopump. Therefore, the boiling flow simulation for liquid oxygen and liquid nitrogen developed thus far was extended to liquid hydrogen as shown in Fig. 2.1. This research activity validated and created a hydrogen boiling model based on good-quality data measured by NASA [9][10][11]. It focused on two-phase flow visualization for checking the mass transfer, and the wall temperature for checking the chilling rate, then compared the simulation and experiment against the liquid hydrogen chill-down process of a vertical pipeline.
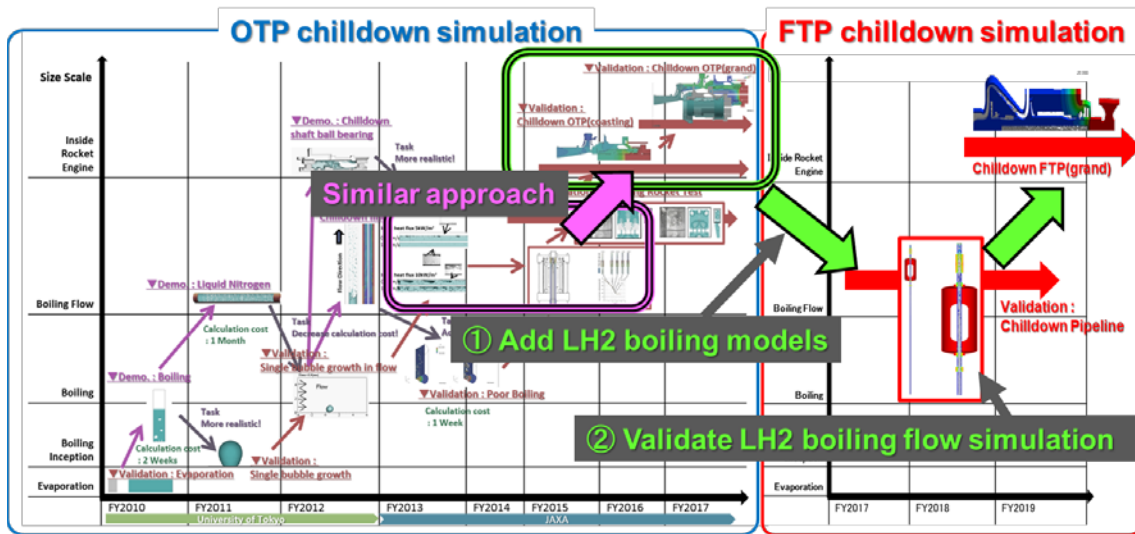

Fig. 2.1. Roadmap of hydrogen chilldown simulation development

III. Experimental Setup and Measurements

A detailed description of the liquid hydrogen transfer line chill-down test setup is available in Ref. [9]; thus, what follows is only a brief description. Testing was performed at the Small Multipurpose Research Facility in Cleveland, OH. Experiments were conducted in a parametric fashion over several inlet liquid temperatures (20.3 K – 24.2 K) corresponding to a range of pressures (101 kPa – 276 kPa), and three flow rates spaced out over 0.0023 kg/s – 0.036 kg/s. Liquid hydrogen was conditioned inside a storage dewar and flow was routed directly to a Coreolis flow meter for liquid flow measurement. The tank and line chill assembly rested inside a vacuum chamber with a thermally controlled cryoshroud that was set to 1.33×10^{-7} Pa and 250 K as shown in Fig. 3.1. Fluid was routed vertically upward through a flow control manifold. Orifices were used to control lower and medium flow rates, while the pipe diameter and driving pressure gradient set the higher flow rate limit. Fluid then passed through a second valve that was common to all three legs. This valve added thermal mass for the system. Flow was then routed vertically upward through a Pyrex sight glass located downstream that was used for real-time flow visualization. Two openings in the canister allowed flow visualization and backlight illumination. Flow was then routed out of the top of the VC lid. The outer diameter of the transfer line was 1.27 cm (0.5 in) and the inner diameter was 1.02 cm (0.402 in). The mass and length of the transfer line, including two valves, orifice, stainless steel (SS) piping, and sight glass were approximately 3.42 kg and 1.62 m, respectively.

Instrumentation is also shown in Fig. 3.1, where SD refers to skin temperature measurement using a wall-mounted silicon diode, PT refers to a pressure reading, and T refers to stream temperature measurement. The transfer line was outfitted with four skin diode temperature sensors (SD16 – SD19) along the main test section. Note

that one diode (SD16) was placed on the outer wall of the valve and another (SD19) was placed along the sight glass wall. The other two skin diodes were mounted directly to the steel portion of the tube. Four internal stream temperature diodes (T5, T6, T15, and T23) were also distributed throughout the experiment. Two diodes (T5 and T6) from the vertical diode rake were used to determine the liquid level and average bulk liquid temperature in the tank at the start of the test. T23 measured internal fluid temperature directly downstream of the sight glass and was used to define when the chill-down test was completed. Finally, four pressure transducers (PTs) (PT1, PT3 – 5) were placed near the temperature sensors. PT1 measured tank ullage pressure, while PT5 measured pressure upstream of the valve manifold. PT3 measured pressure downstream of the valve manifold but upstream of the sight glass, while PT4 measured pressure directly downstream of the sight glass.

The methodology for conducting a line chill test was as follows: the background vacuum chamber pressure was set to 1.33×10^{-7} kPa and the cryoshroud temperature was set to 250 K. The storage tank was then filled with LH_2 and conditioned to the desired saturation temperature. Once the liquid was conditioned, the tank was pressurized with gaseous helium (GHe) to the desired total tank pressure in order to subcool the liquid. After the transfer line was sufficiently chilled and a steady-state condition achieved, testing would cease. After testing was completed, externally mounted heaters would warm the hardware back to the initial temperature of 250 K for the next test.
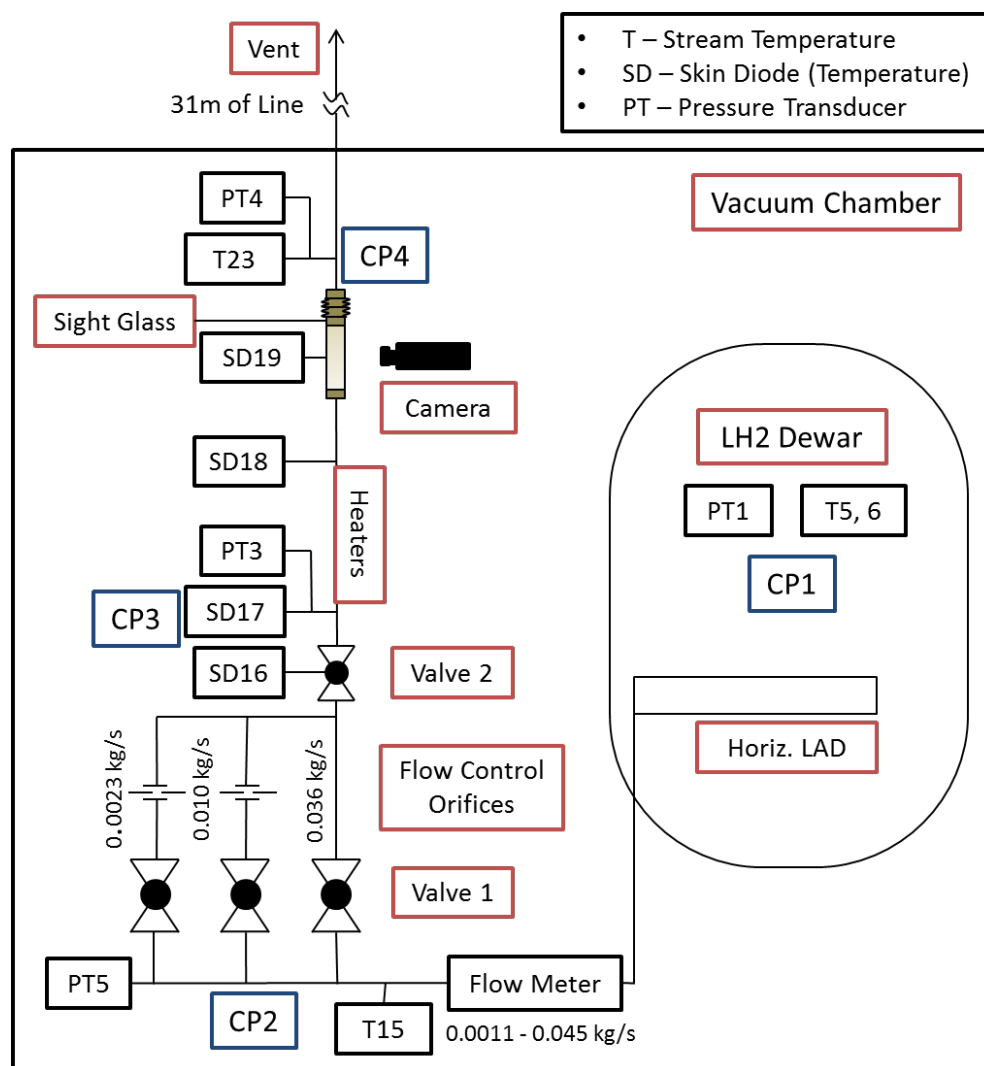
Fig 3.1 Experiment schematic

American Institute of Aeronautics and Astronautics

IV. Numerical formulations

To predict variations in the cooling effect under microgravity, a numerical method is needed to indicate differences in the boiling flow pattern through the existence of buoyancy. As this requires the reproduction of the union and division of a bubble, research has been conducted toward creating a prediction tool based on a numerical method for free surface flows. To predict the motion of a liquid, the University of Tokyo and JAXA have developed the CIP-based Level Set & MARS (CIP-LSM), which combines the VOF and the level-set method as an analysis technique with high mass conservation [2][3][4]. For calculations that consider gaseous compressibility or surface tension, CIP-LSM offers a stable and robust means of performing calculations with density ratios as large as 1000. During the research process, a numerical model for considering the phase change at the liquid surface was developed and implemented in CIP-LSM [5][6][7]. The governing equation and phase change model in the simulation tool are explained below.

By assuming local equilibrium, the governing equations (i.e., equation of continuity, conservation laws for momentum and energy) for a phase change can be described as follows:

$$\rho \frac{D\vec{u}}{Dt} = -\nabla p + \nabla \cdot (\mathbf{T}_v + \mathbf{T}_\sigma) + \vec{F} + (\vec{u}_{Gas} - \vec{u}_{Liq.})\dot{m}\delta_S \tag{4.1}$$

$$\rho C_p \frac{DT}{Dt} = -T \frac{1}{\rho} \frac{\partial \rho}{\partial T}\Big|_p \frac{Dp}{Dt} + \dot{\Theta} \tag{4.2}$$

$$\frac{1}{\rho C_S^2} \frac{Dp}{Dt} = -\nabla \cdot \vec{u} - \frac{1}{\rho}\frac{\partial \rho}{\partial T}\Big|_p \frac{\dot{\Theta}}{\rho C_p} - \left(\frac{1}{\rho_{Gas}} - \frac{1}{\rho_{Liq.}}\right)\dot{m}\delta_S \tag{4.3}$$

$$\dot{\Theta} = \{(\mathbf{T}_v + \mathbf{T}_\sigma) \cdot \nabla\} \cdot \vec{u} - \nabla \cdot \vec{q} - (h_{Gas} - h_{Liq.})\dot{m}\delta_S \tag{4.4}$$

$$\mathbf{T}_v = \left[\tau_{ij}\right] = \lambda(\nabla \cdot \vec{u})\mathbf{I} + \mu(\mathbf{D} + \mathbf{D}^T) \tag{4.5}$$

$$\mathbf{T}_\sigma = \sigma\delta_s(\mathbf{I} - \vec{n}_s\vec{n}_s) \tag{4.6}$$

To distinguish the gas phase from the liquid phase, CIP-LSM adapts the Heaviside function, H_s[-] which is defined as follows:

$$
\begin{aligned}
H_s &= \quad 0.5 \ : \ \text{the fluid is in the liquid state} \\
H_s &= \quad 0.0 \ : \ \text{the point is located on the liquid surface} \\
H_s &= \ -0.5 \ : \ \text{the fluid is in the vapor state}
\end{aligned}
\tag{4.7}
$$

So, the density can be written as

$$\rho = (0.5 - H_S)\rho_{Gas} + (0.5 + H_S)\rho_{Liq.} \tag{4.8}$$

The change in the Heaviside function in the flow field is described by two convection equations that distinguish the gas phase from the liquid phase as follows:

$$\frac{\partial H_S}{\partial t} + \vec{u}_S \cdot \nabla H_S - \frac{\dot{m}}{\rho_{Gas}}\vec{n}_S \cdot \nabla H_S = 0 \tag{4.9}$$

$$\frac{\partial H_S}{\partial t} + \vec{u}_S \cdot \nabla H_S - \frac{\dot{m}}{\rho_{Liq.}}\vec{n}_S \cdot \nabla H_S = 0 \tag{4.10}$$

In addition, the equation of state for each phase is used as a governing equation. In this research, numerical handling of the gas-liquid interface was defined in order to consider a phase change. In the model, the area that assumes a thermal balance was sufficiently small, as shown in Fig. 4.1, so that even in a non-equilibrium situation, it attained equilibrium in a short time relative to a computational time unit. As a result, it was deemed unnecessary to consider the time lag for a state-change.

Information about temperature and pressure saturation could be acquired from a saturated vapor pressure curve using Antoine's equation. From the relationship between the latent heat relative to the saturation temperature, and the difference in the speed of propagation, the saturation temperature was calculated from Antoine's equation, with pressure being used as a parameter in this model as follows:
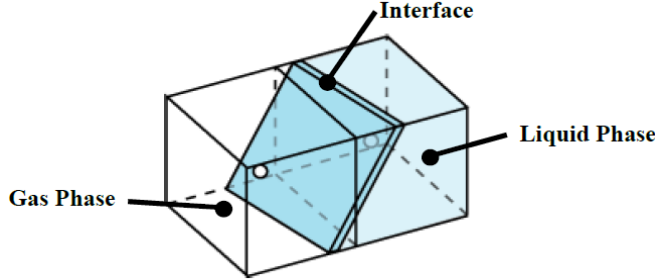
$$T_{sat} = \frac{B}{A - \log_{10} p} - C \tag{4.11}$$

Latent heat was calculated from the following equation derived from the Clausius-Clapeyron equation and Antoine's equation:

$$L = \{B(A - log_{10}\, p) - C(A - log_{10}\, p)^2\} \times \left(\frac{1}{\rho_{Liq.}} - \frac{1}{\rho_{Gas}}\right)\frac{p\, ln\, 10}{B} \qquad (4.12)$$

Table 4.1 below lists the constants used in Eqs. (4.11) and (4.12).

Figure 4.1. Relationship between computed grid and gas-liquid interface

Table 4.1.   Antoine constants

Antoine constants	H_2
A	7.9395
B	66.795
C	2.5000

In this model, the rate of phase change per unit area $\dot{m}$ [kg/m2/s] was calculated from the following equation:

$$\dot{m} = \frac{\left(\vec{q}_{Liq.} - \vec{q}_{Gas}\right)\cdot\vec{n}}{L} \qquad (4.13)$$

The velocity jump was calculated using the following equation

$$\vec{u}_{Liq.} - \vec{u}_{Gas} = \dot{m}\left(\frac{1}{\rho_{Liq.}} - \frac{1}{\rho_{Gas}}\right)\vec{n} \qquad (4.14)$$

Equations (4.13) and (4.14) indicate a jump in the normal direction to a gas-liquid interface. These vectors form the flux of the non-conservative governing equations of energy and continuity, and act as conditions of the junction between the liquid and vapor phases. This model assumes that a gas-liquid interface exists between the two cells. Under this assumption, by substituting Eqs. (4.13) and (4.14) into the governing equations, equations that include flux jump as an immersed-boundary method were obtained. In this model, the diffusion equation was solved using the saturation temperature at the gas-liquid interface, $\dot{m}$ [kg/m^2/s] was calculated from the temperature gradient with Eq. (4.13), Poisson's equation was calculated with Eq. (4.14) and the gas-liquid interface position was updated using Eqs. (4.9) and (4.10).

V.   Numerical Model of Boiling

It is impractical in terms of calculation cost to resolve the gas-liquid interface of a small bubble into several cells in chill-down simulations of a turbo-pump. Therefore, JAXA developed a sub-grid-scale model for calculating boiling inside a cell [7][8]. This model considers both the volume change and latent heat according to bubble growth inside a cell in order to cooperate with the analysis of both fluid dynamics and heat transfer.

In this model, boiling inception was reproduced by two processes. Bubble growth according to Eq. (5.2) would start when the degree of superheating was greater than ΔT_{SH} [K], as calculated using Eq. (5.1) for cavity size r_{cavity} [mm], which was obtained from the surface roughness. Equation (5.2) derived from integration over a bubble surface as shown in Fig. 5.1 could calculate the bubble growth rate. Equation (5.3) calculated the amount of evaporation on the bubble surface, $\dot{m}$ [kg/m^2/s].

$$\Delta T_{SH} = \frac{2\sigma\left(\frac{1}{\rho_{Gas}} - \frac{1}{\rho_{Liq.}}\right)T_{sat}}{L}\frac{1}{r_{cavity}} \qquad (5.1)$$

$$\dot{V} = \frac{1}{\rho_{Gas}}\oint_{Bubble}\dot{m}(\varphi)dS(\varphi)$$
$$= \frac{2\pi k_{Liq.}\left(T_w - T_{sat}\right)r}{\rho_{Gas}L}log\frac{cos\,\theta}{cos\,\theta - \varepsilon} \qquad (5.2)$$

$$\dot{m}(\varphi) = \frac{k_{Liq.}(T_w - T_{sat})}{Lr(\cos\theta - \cos\varphi)} \qquad (5.3)$$

where T_w [K] denotes the temperature of the wall surface, θ [rad] is the contact angle, r [m] is the bubble radius, and ε [-] is a parameter of minimum liquid film thickness.

In this sub-grid-scale model, the number of bubbles generated in the cell is very important because Eq. (5.2) only calculates the growth of a single bubble. Thus, the number of bubbles increases the volume change and latent heat in a cell. The boiling curve is reproduced by modeling the size and number of cavities on the heating surface in JAXA's simulation tool. It was important to model the dryout to reproduce the transition to the spray flow in a development of hydrogen chill-down simulation.
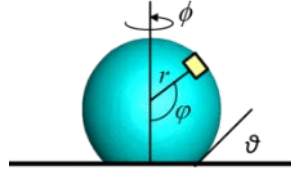

Fig. 5.1. Definition of a coordinate axis at a bubble on the heating surface

VI. Results and Discussion

In order to reproduce the liquid hydrogen vertical pipeline chill-down experiment conducted by NASA, simulation from downstream of the valve opened at the test start to the test section outlet was necessary as chill-down occurred in a wide section due to the high cooling effect of the hydrogen spray flow as revealed in the simulation results. The simulation results introduced in this paper used the computational domain shown in Fig. 6.1, and were modeled in order to solve the heat transfer of the pipeline and fluid conjugately. In Fig. 6.1, the region belonging to the fluid simulation is colored blue.

The initial calculation condition for both fluid and pipeline was 250 K as the temperature was controlled by the heater in the experiment. The mass flow rate at the inlet and the pressure at the outlet were experimental data used as boundary conditions. Other boundary conditions are described in Fig. 6.2.
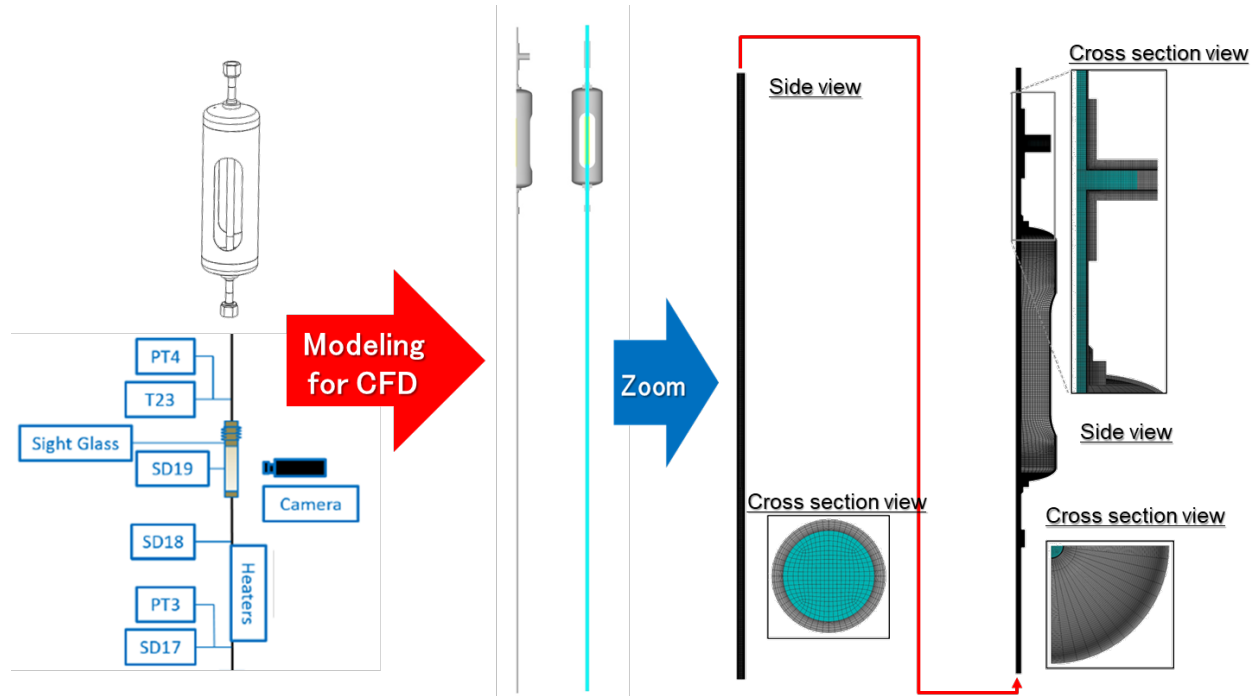
Fig. 6.1. Computational domain for NASA's liquid hydrogen chill-down pipeline test

American Institute of Aeronautics and Astronautics
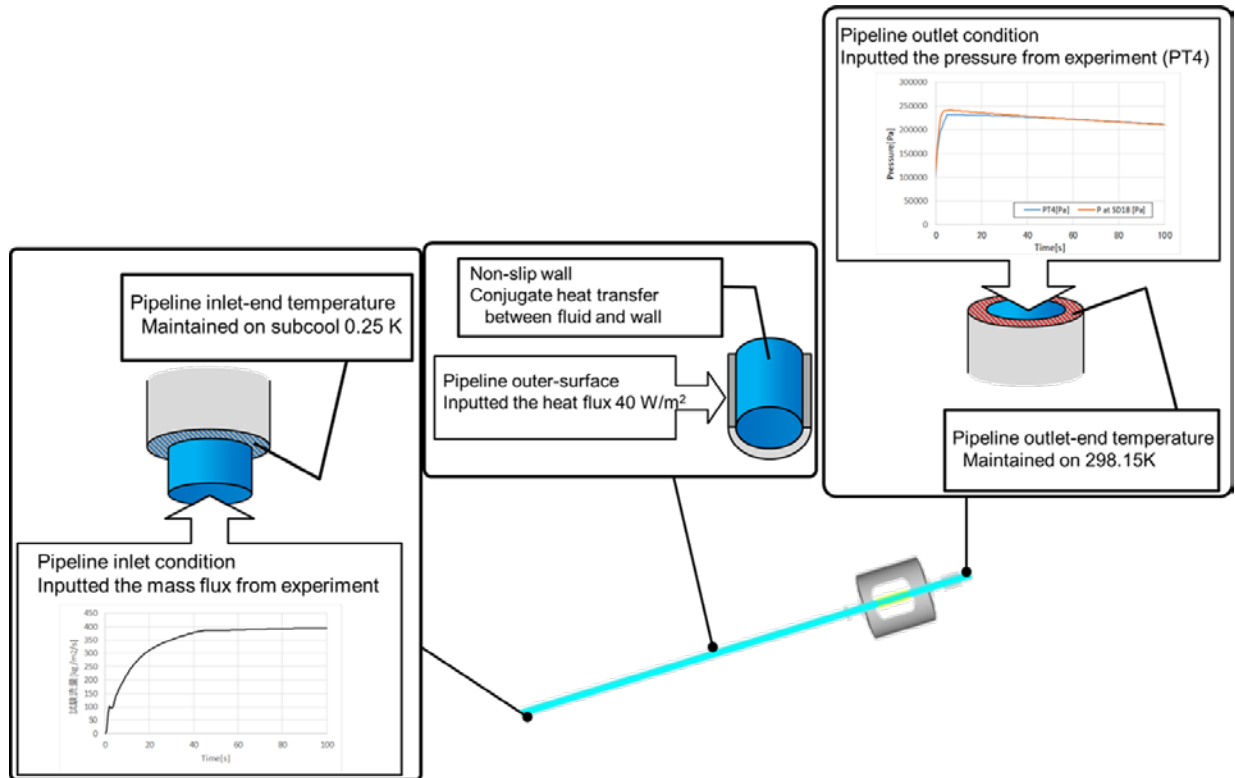
Fig. 6.2. Boundary conditions for NASA's liquid hydrogen chill-down pipeline test

Figure 6.3 also shows the temperature time histories of each part. In this graph, a solid line indicates a simulation result, and a dash line indicates an experimental result. The time responsiveness of the visualization section showed good agreement between the test and CFD as indicated by the red lines. Conversely, the surface response temperature of the upstream pipeline made of metal is somewhat different in time response as indicated by the blue lines. Figure 6.4 shows the relationship between the fluid temperature inside the pipe and the pipe's surface temperature for discussing the upstream pipeline temperature difference between the simulation and experiment. This graph indicates that the time response of the fluid temperature and upstream piping surface temperature show good agreement. These results suggest a difference between the simulation and experiment in terms of the pipe surface temperature time history, depending on the liquid ratio reached at the test start and the initial pipeline temperature distribution. However, good agreement was shown regarding the surface temperature time history of the test section as there was no uncertain information, such as reaching the liquid ratio in the test section and regarding the initial temperature distribution.

The green lines in Fig. 6.3 show the fluid temperature at the visualization zone exit. The timings at which the fluid temperature rises and falls coincide, but were somewhat different for the quantitative temperature evaluation. The predicted performance of the thermal flow inside the test section was confirmed as not causing the difference in temperature downstream of this test section between the experiment and simulation. This temperature history was mainly due not only to the connecting point of the shield but also to the flow channel geometry used for installing the temperature and pressure sensors. Figure 6.5 shows the basis for discussing the relationship between this temperature history and the flow. Figure 6.5 (a) indicates the velocity distribution, and (b) indicates the temperature distribution. The triangular mark in Fig. 6.5 (c) indicates the point at which nucleate boiling occurs. It could be confirmed from Fig. 6.5 (a) that the fluid velocity at the test section outlet decreases, although the mass flow rate into the pipeline increases with the passage of time. This phenomenon was caused by the lower evaporation generated in the upstream pipeline due to chill-down. This mechanism could be confirmed from the facts that the nucleate boiling zone approached the test section and the liquid ratio increased as shown in Fig. 6.5 (c). This simulation was modeled based on the pipe union and the cross for sensor installation. It could be confirmed from Fig. 6.5 (b) that the fluid temperature in this flow channel changes according to the flow velocity and liquid ratio. From the above, the outlet fluid temperature tends to decrease due to the cooling that depends on the steam flow in five seconds and the spray flow after ten seconds. However, the drop in temperature is temporarily stopped because the

American Institute of Aeronautics and Astronautics

flow velocity decreases when the liquid rate changes due to chill-down of the upstream pipeline. As shown in these results, as well as in the conditions of liquid hydrogen, it was confirmed that this simulation could be used for a quantitative prediction of temperature and an investigation of phenomena inside the flow channel as shown in Fig. 6.6.
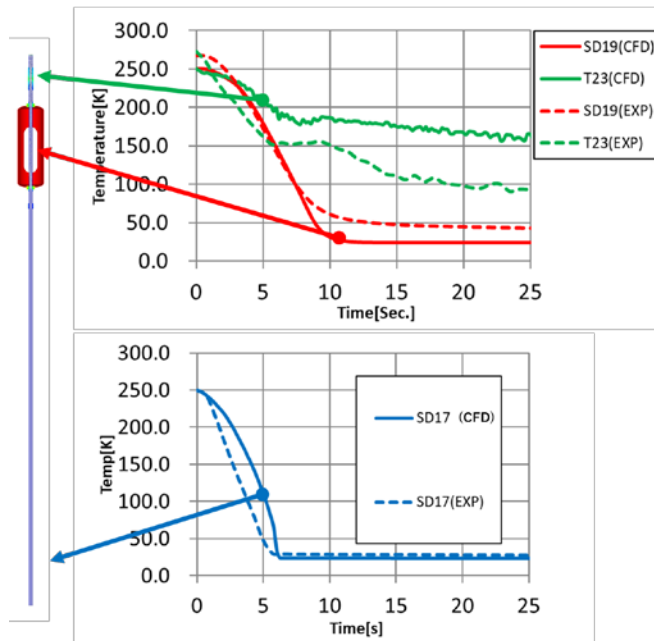
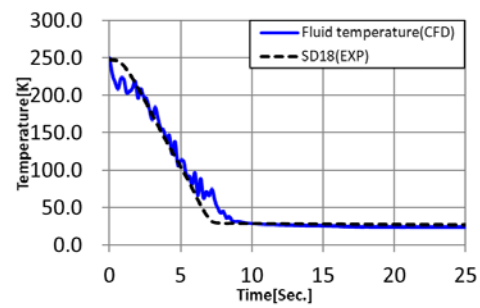

Fig. 6.3. Comparison of temperature histories

Fig. 6.4. Fluid temperature correspondence in upstream pipeline

(a) Velocity distribution

(b) Temperature distribution
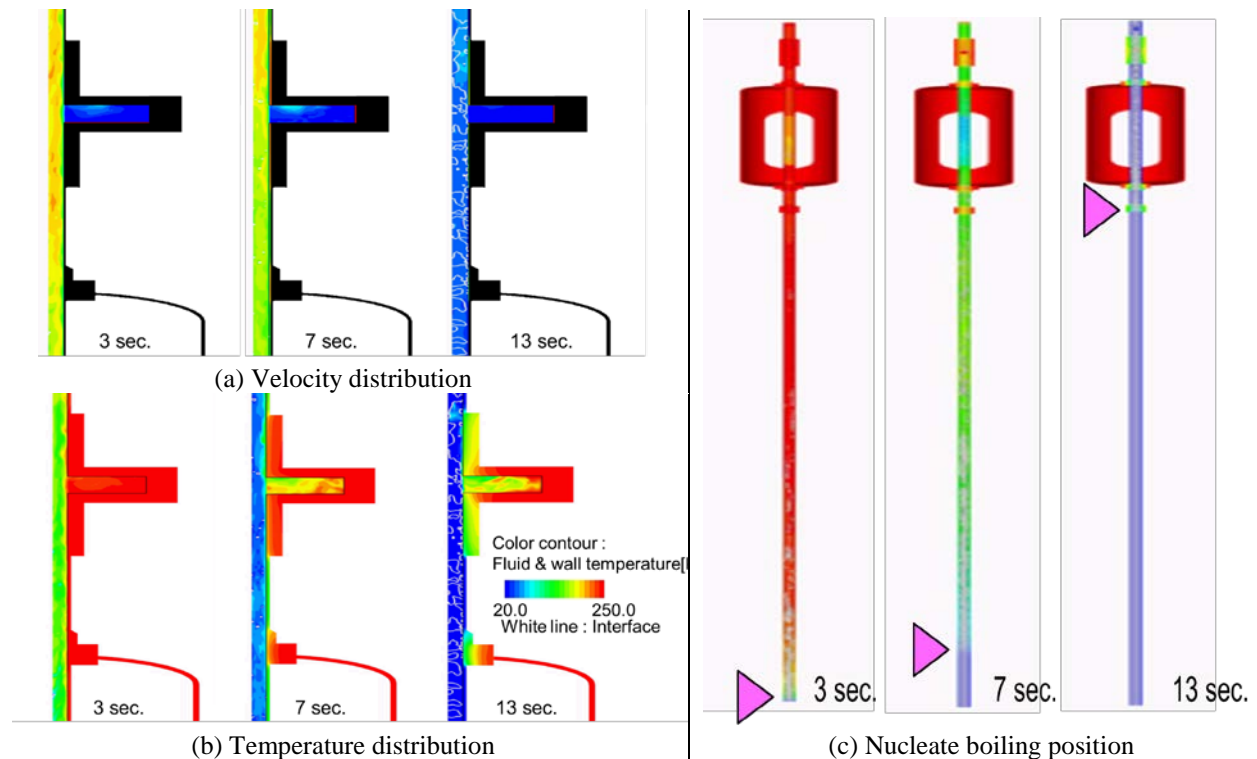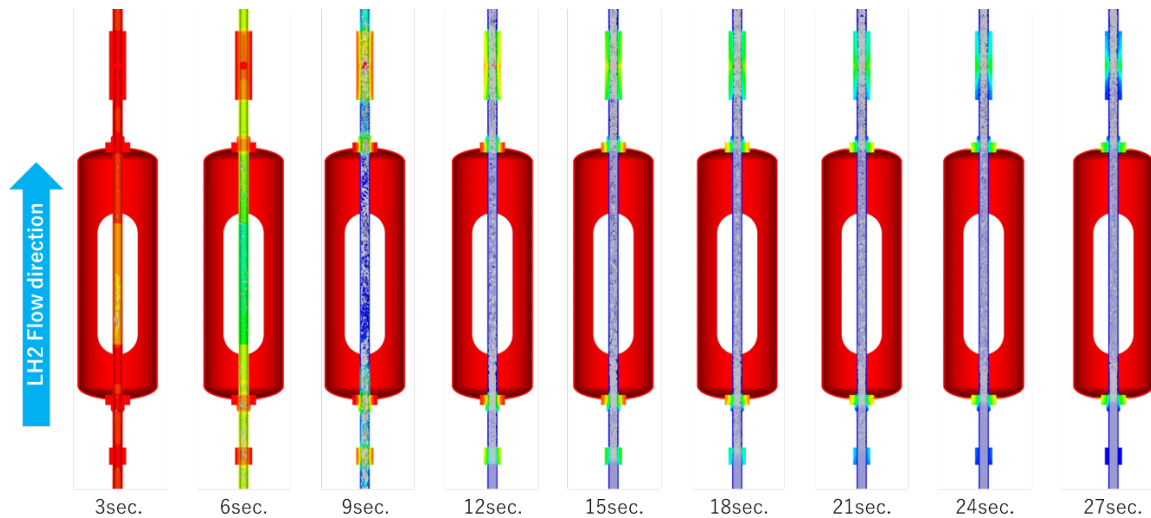

(c) Nucleate boiling position

Fig. 6.5. Thermal flows inside the pipe union and the cross for sensor installation

Fig. 6.6. Two-phase flow numerical visualization and temperature distribution at the test-section

VII. Summary

JAXA has aimed to upgrade such propellant management technologies as the multiple ignitions of an engine in response to the demands for "orbital transportation by large impulse" and "cost reduction" regarding the development of next-generation cryogenic liquid rockets. In one technology improvement activity, turbopump chill-down simulation was expected to aid in understanding internal flow during engine re-ignition. Thus, JAXA aimed to realize an evaluation technology for the liquid hydrogen chill-down process by using and applying the experience and knowledge gained from simulation tool development in the H-IIA upgrade project. Hydrogen boiling simulation was validated in collaborative research with the NASA Glenn Research Center. The results of said validation confirmed that liquid hydrogen chill-down simulation could be used for a quantitative prediction of temperature and an investigation of phenomena inside the flow channel.

JAXA has obtained the chill-down estimation of a liquid hydrogen turbopump for a reusable rocket engine as the outcome of this collaborative research. JAXA has researched reusable liquid rockets since 1998, and development is currently underway for a 100-km altitude flight test in 2020. This liquid hydrogen turbopump simulation was conducted to grasp the boiling flow phenomenon from engine cut-off to re-ignition. The simulation results revealed such aspects of the boiling flow phenomenon as the occurrence of bumping at engine cut-off due to a saturation temperature lower than the working fluid temperature caused by a drop in pump pressure, as shown Fig. 7.1, and dry out being caused by flow due to the pressure loss balance around the pump bearing. And as shown in Fig. 7.2, the scale of dryout was confirmed by CFD as being different depending on the direction of gravity.

The activity results introduced in this paper are only one of the themes of collaborative research between JAXA and the NASA Glenn Research Center. This joint research has the potential to develop into an international cooperative relationship for discussing the cryogenic propellant management technologies necessary to achieve manned Mars exploration and other future missions.
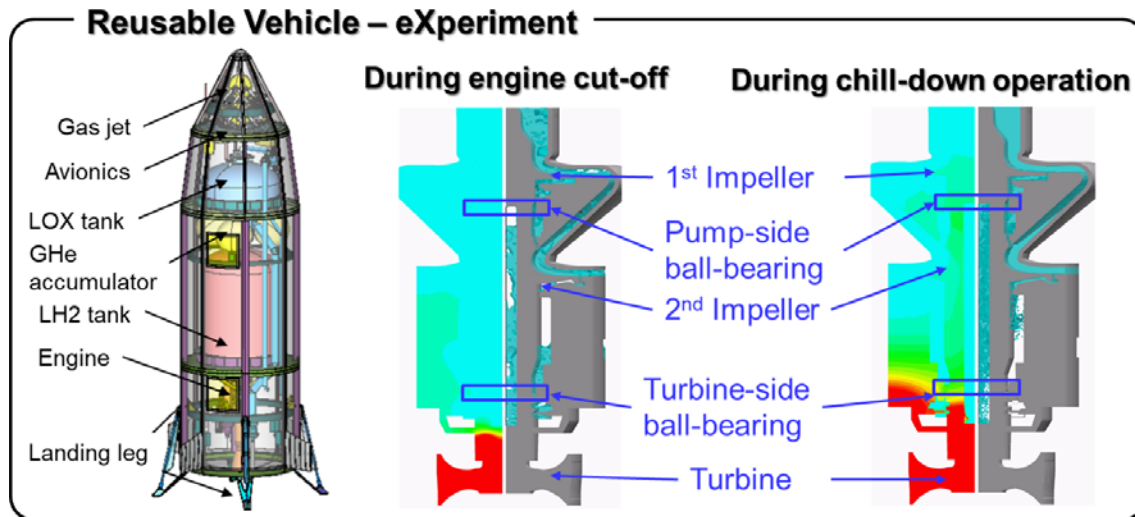
American Institute of Aeronautics and Astronautics

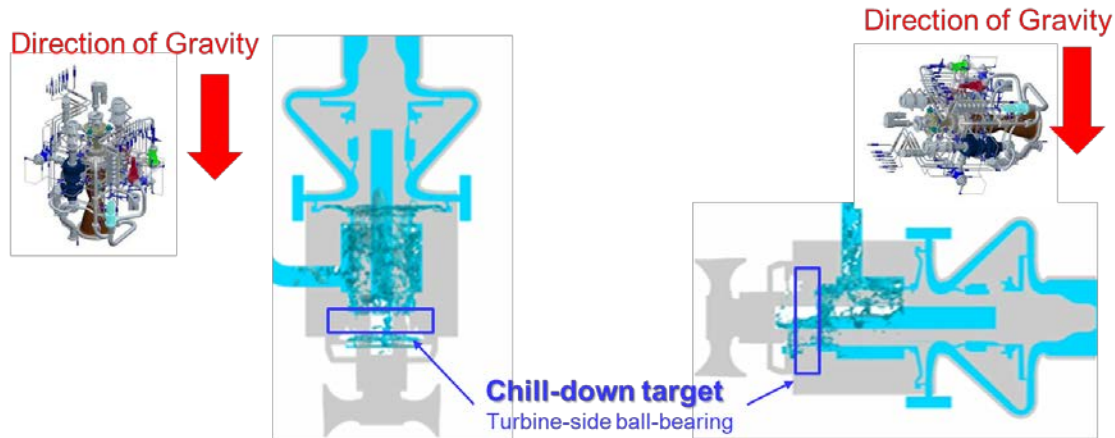**Fig. 7.1. Boiling simulation inside an engine for JAXA's reusable liquid rocket development**

Fig. 7.2. Effect of gravity direction during a chill-down process

References

[1]   Niitsu M., Yasui M., Shimura Y., Yabana J., Tanabe Y., Ishikawa K., H-IIA Launch Vehicle Upgrade Development - Upper Stage Enhancement to Extend the Lifetime of Satellites -, Mitsubishi Heavy Industries Technical Review Vol. 51 No. 4 (2014).

[2]   Himeno T., Watanabe T. and Konno A., Numerical Analysis of Two-phase Flow Behavior in a Liquid Propellant Tank, AIAA 99-2177, (1999).

[3]   Himeno T., Negishi H., Nonaka S., Inoue C., Watanabe T. and Uzawa S., Transaction of the Japan Society of Mechanical Engineers, B76(765), pp.778–788.

[4]   Himeno T., Proceeding of the conference on computational engineering and science, Vol.13(2), pp789–792.

[5]   Umemura Y., Himeno T. and Watanabe T., Journal or Japan Society of Fluid Mechanics, Vol.20(2), pp.79–85.

[6]   Umemura Y., Himeno T., and Watanabe T., AIAA ASME SAE ASEE Jt Propuls Conf Exhib, 49th Vol. 4, pp2673-2686.

[7]   Umemura Y., Himeno T., Kinefuchi K, Tani N., Negishi H., Kobayashi H.Ohira K. and Fukasawa O., AIAA ASME SAE ASEE Jt Propuls Conf Exhib, 51st, pp2015-3855.

[8]   Umemura Y., Himeno T., Osamu K., Sarae W., Kobayashi H., and Fukasawa O., AIAA SAE ASEE Jt Propuls Conf Exhib, 53st, pp2017-4761.

[9]   Hartwig, J.W., Styborski, J., McQuillen, J., Rame, E., Chung, J. "Liquid Hydrogen Line Chilldown Experiments: Optimal Chilldown Methods" International Journal of Heat and Mass Transfer 137, 703 – 713. 2019.

[10]   Jason Hartwig, Samuel Darr, Anthony Asencio, International Journal of Heat and Mass Transfer 93 (2016) 441–463.

[11]   Jason Hartwig, Enrique Rame, John McQuillen, AIAA 2016-2186.